Understanding and controlling the weakly interacting interface in perylene/Ag(110)

L. Gao, Z. T. Deng, W. Ji, X. Lin, Z. H. Cheng, X. B. He, D. X. Shi, and H.-J. Gao*
Institute of Physics, Chinese Academy of Sciences, P.O. Box 603, Beijing 100080, China
(Received 28 August 2005; revised manuscript received 9 January 2006; published 16 February 2006)

The weakly interacting interface, perylene on Ag(110), has been systematically investigated in detail with molecular-beam epitaxy and low-energy-electron diffraction (LEED), low-temperature-scanning-tunneling microscopy (STM), and first-principles calculations. The overall process of perylene monolayer growth has been clearly discussed by LEED and STM. The monolayer structure is sensitive to growth conditions because perylene has a poor self-assembly ability on Ag(110). However, we achieved the control of the formation of the uniform perylene monolayer composed of only one superstructure. The locally distributed metastable structures produced on certain growth conditions were also discussed.

DOI: 10.1103/PhysRevB.73.075424 PACS number(s): 68.37.Ef, 68.43.Bc, 68.43.Fg

I. INTRODUCTION

The investigation of various organic/metal interfaces is currently attracting considerable interest.[1–6] While organic multilayer is practically applied in organic electronics and optoelectronics, the organic/metal interfaces play a crucial role in the performance of the molecular devices.[7–19] Self-assembly is one of the few practical "bottom-up" methods to prepare organic nanostructures. Previous work on molecular self-assembly shows that the molecular adsorption configurations are strongly affected by the surface structure of the substrate and the balance between intermolecular interaction and molecule-substrate interaction. In some cases, surface structure can serve as a template for the formation of one- or two-dimensional molecular nanostructures.[4,5,20] In other cases, the molecular self-assembly on flat and unstructured surfaces can be realized by strong molecule-substrate interaction or intermolecular interaction.[1,21] All the cases mentioned above have strong self-assembly ability that easily leads to the formation of crystalline structures. However, for a large proportion of organic/metal systems, the molecule-substrate interaction, the intermolecular interaction and the template-influence of the substrate are all quite weak; hence the fabrication of highly ordered molecular nanostructures is quite sensitive to growth conditions due to the lack of internal dominating driving force for self-assembly.[3,22] These systems can therefore be classified as weakly interacting. Decorating the molecules with functional groups can effectively enhance molecule substrate or intermolecular interaction; thereby molecular self-assembly with a high degree of order can be realized.[23,24] However, the electronic or optoelectronic properties of the molecules are changed accordingly. Therefore, understanding and controlling the self-assembly for the weakly interacting system are significant in organic electronics and optoelectronics.

Perylene ($C_{20}H_{12}$) and its derivatives have attracted considerable interest in recent years because of their excellent performance in electronic[17,25] and light emitting devices.[16,26–28] Considerable studies of the growth of perylene crystals[29] and thin films[30–32] have been reported. Previous studies on perylene/metal interfaces show that perylene molecules have strong interaction with Cu(110),[31,32] whereas weak interaction with Ag(111)[22] and Ag(110).[30] Considering the fact that organic semiconductors on single-crystalline metal surfaces are typical systems for injection contacts in OFETs and OLEDs, and that silver has a relatively high work function (4.52eV), we select Ag(110) as the substrate in our experiment.

The adsorption of perylene on Ag(110) has been investigated with molecular-beam expitaxy (MBE) and low-energy-electron-diffraction (LEED).[30] In Ref. 30, the authors demonstrated the transition of the LEED pattern during the growth of perylene on Ag(110). One final superstructure and one intermediate superstructure were determined by LEED, and three other superstructures were observed but not discussed in detail. Perylene forms several superstructures under slightly different growth conditions, which indicates that the perylene/Ag(110) interface has poor self-assembly ability. Nowadays, scanning tunneling microscope (STM) has been widely used in studying organic/metal interfaces. In comparison with LEED, STM has a much higher space resolution, which allows investigating the nanostructures at single molecular level. STM can detect the local properties, such as steps, dislocations, locally distributed structures, defects, domain boundaries, etc. In addition to this, high-resolution STM imaging helps to identify the molecular configurations in combination with first-principles calculations, which is beyond the capability of LEED. Therefore, investigation with STM is necessary to understand in depth the perylene/Ag(110) interface. In the present paper, we investigate the perylene/Ag(110) interface with low temperature (LT) scanning tunneling microscopy and LEED. To our knowledge, no STM results on perylene/Ag(110) have been reported before. Submonolayers at three typical coverages are discussed in detail. By finely controlling the growth conditions, we obtained one perylene monolayer composed of single superstructure different from those reported in Ref. 30, with few defects and rather large domain size. First-principles calculations are conducted to identify the molecular configuration and calculate the adsorption energy.

II. EXPERIMENTS

All the experiments were performed with an Omicron UHV MBE-LTSTM system with a background pressure be-

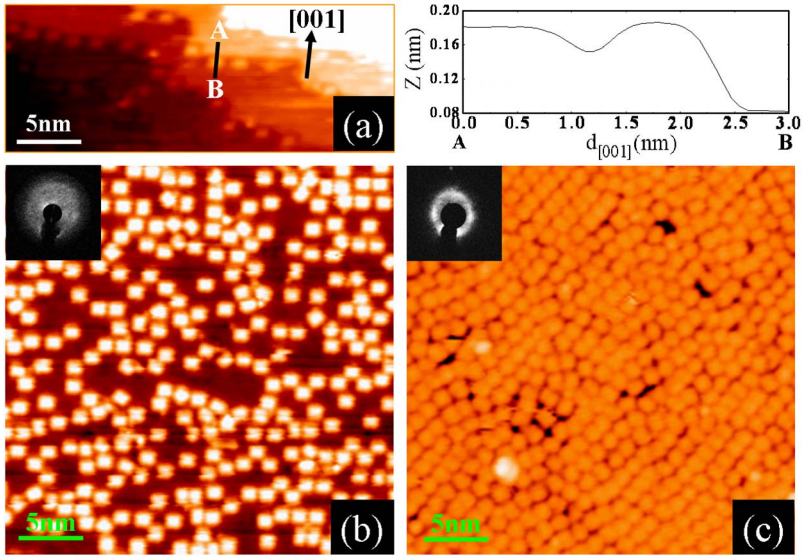

FIG. 1. (Color online) (a) STM image (30 nm×12 nm, $U=-1.7$ V, $I=0.09$ nA) of the initial adsorption stage of perylene on Ag(110) surface. The attached curve is the line profile (from A to B in STM image) across a molecule adsorbed along the [001] step edge. (b) STM image (35 nm×35 nm, $U=-1.8$ V, $I=0.04$ nA) showing the scenario after one submonolayer, with a molecular coverage of 3.1×10^{13} molecules per cm^2, was cooled down to 7 K. The inset shows the LEED pattern (12 eV) of this sample. (c) STM image (35 nm×35 nm, $U=-1.7$ V, $I=0.11$ nA) showing the scenario after another submonolayer, with a molecular coverage of 4.6×10^{13} molecules per cm^2, was cooled down to 77 K. The inset shows the LEED pattern (12eV) of this sample.

low 3.0×10^{-10} mbar. The Ag(110) surface was cleaned by repeated cycles of Ar^+ sputtering (1keV, $Ar^+5.9\mu A/cm^2$) and subsequent annealing to 700K. Then the cleanliness of the surface was checked by LEED and LT-STM. Perylene (Acros, 99+%) materials were effectively purified using the temperature gradient sublimation method[33] and immediately loaded into the sublimation cells. The cells were kept at 338K for 24 h to be degassed thoroughly before evaporation experiments.

The evaporation experiments were conducted with MBE-LEED (Refs. 3 and 34) which allows *in situ* recording of diffraction patterns in real time during molecular deposition. The electron energy is set at 12 eV to record the LEED pattern during the adsorption of perylene on Ag(110) surface. The LEED pattern appears like a halo at dilute coverage, changes into a diffuse ring with the coverage increasing, then decays into diffuse spots with the coverage close to one monolayer, and finally shows sharp diffraction spots at monolayer coverage. We define a monolayer with a molecular coverage of about 5.0×10^{13} molecules per cm^2.

All the STM experiments were performed with the Omicron LT-STM. Perylene molecules cannot be clearly imaged with STM at room temperature at both submonolayer and monolayer coverage due to the high molecular mobility on the silver surface. Therefore, it is necessary to conduct STM scanning at lower temperatures where the molecules have rather low mobility. Therefore, after the sample was prepared, it was cooled down very slowly to low temperatures. All the STM measurements were conducted at low temperatures using a chemically etched tungsten tip that was carefully cleaned before any measurements. For our STM, the voltage bias refers to the sample with respect to the tip. All the STM images in this paper were recorded in a constant current mode.

III. RESULTS AND DISCUSSION

A. Submonolayer

After a small number of perylene molecules were deposited onto the silver surface at 320 K, as shown in Fig. 1(a), most of the molecules adsorb on step edges, while only a few molecules were observed on terraces, which indicates that the sites at step edges on Ag(110) are more active, compared with the sites on terraces, for the adsorption of perylene at 77 K. All molecules along step edges lie below step risers in the form of isolated molecules without uniform intermolecular distance. Under typical tunneling conditions $U=-1.3$ V and $I=0.09$ nA, the apparent height of the molecules is about 1 Å, roughly equals the height of a Ag(110) step. There is a depression of about 0.4Å between molecules and the silver layer above the step risers, as indicated by the line profile from A to B in Fig. 1(a). The configuration of the molecules adsorbed on step edges is different from the "flat-flying" configuration on terraces due to the existence of the microfacets at steps edges.

Surface steps, in many cases, are the preferential adsorption sites for molecules.[35–37] Benzene molecules prefer to adsorb on $[1\bar{1}0]$ step edges on Ag(110) surface.[35] Pascual *et al.* explain that the [001] step edges are less active adsorption sites than the $[1\bar{1}0]$ step edges due to their different electronic structures. In our experiments, however, perylene molecules can be observed on both [001] and $[1\bar{1}0]$ step edges. So the existence of a gap in the density of states at the Fermi level,[38,39] which is believed to be responsible for the preferential adsorption of benzene on $[1\bar{1}0]$ step edges on the Ag(110) surface,[35] does not induce similar adsorption preference between [001] and $[1\bar{1}0]$ steps of the Ag(110) surface for perylene.

The diffuse halolike LEED pattern appears and expands from the center when the coverage further increases; see the inset of Fig. 1(b). The expansion of the halo is the result of increasing the coverage and thus decreasing the average intermolecular distance. Figure 1(b) is a typical STM image showing the scenario after the sample was cooled down to 7 K. The submonolayer was fabricated by depositing about 3.1×10^{13} molecules per cm^2 on the substrate at 320 K. It can be seen that all the molecules distribute on the silver surface homogeneously and disorderly at this coverage. Extensive STM images show that the molecules on step edges

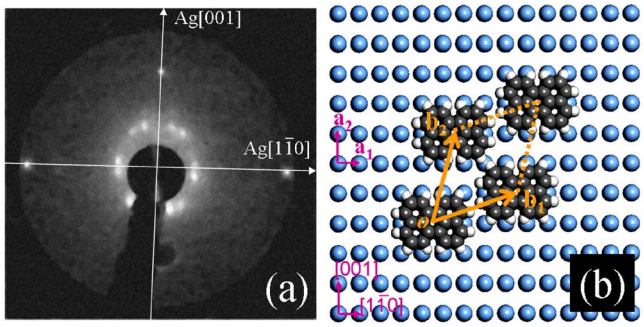

FIG. 2. (Color online) (a) LEED pattern of a highly ordered perylene monolayer. The beam energy is 33 eV. The diffraction spots of the perylene superstructure are symmetric with respect to the two directions indicated in the image. (b) The structural relation between the perylene superstructure and the silver substrate in real space. The adsorption sites of perylene molecules are arbitrarily chosen. $\mathbf{b}_1=4\mathbf{a}_1+\mathbf{a}_2$, $\mathbf{b}_2=\mathbf{a}_1+3\mathbf{a}_2$, $\mathbf{b}_1=16$ Å and $\mathbf{b}_2=15$ Å.

do not act as capturing nucleus for further growth from steps during the cooling process because no condensed molecular islands are observed near steps. On terraces, molecules do not aggregate into condensed molecular islands either. This growth mode is ascribed to the weakness of intermolecular interaction, and typical for weakly interacting systems.

Further increasing the coverage, the diffuse halolike LEED pattern changes into the diffuse ringlike pattern, and then evolves into several bright divisions, as shown in the inset of Fig. 1(c). The brightness division at higher coverage indicates that the disordered distributing of the molecules gradually evolves into quasiordered arrangement. Figure 1(c) shows a typical STM image of the scenario after the sample was cooled down to 77 K, a much higher temperature than that for Fig. 1(b) due to the depression of lateral diffusion of molecules at higher coverage. The submonolayer was fabricated by depositing about 4.6×10^{13} molecules per cm^2 on the substrate at 320 K. Figure 1(c) shows that the molecules are in a quasi-ordered arrangement with a high density.

B. Monolayer

Highly ordered perylene monolayer was fabricated by evaporating about 5.0×10^{13} molecules per cm^2 onto the Ag(110) surface at 320 K. The structure of the monolayer was determined by analyzing LEED pattern at room temperature and high-resolution STM images at 77 K. To capture the diffraction spots of the perylene superstructure and those of the silver substrate in one picture, the electron energy was increased up to 33 eV. Figure 2(a) shows the captured LEED pattern, including twelve diffraction spots of perylene superstructures and four of silver substrate. The molecular superstructure has two domain orientations mirrored at the crystal axis of the Ag(110) substrate, which is induced by the two-fold symmetry of the substrate. The rather high molecular mobility at room temperature induces a rather large Debye Waller factor that causes a significant attenuation of the diffraction spots. Approximately, a commensurate superstructure is determined by the LEED pattern

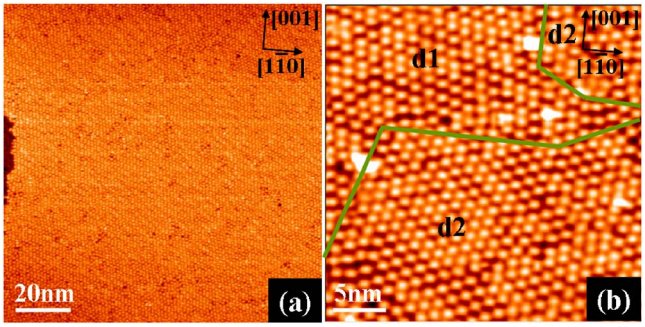

FIG. 3. (Color online) (a) STM image (115 nm×115 nm, $U=-1.7$ V, $I=0.08$ nA) of the highly ordered perylene monolayer without any domain boundaries. (b) High-resolution STM image (30 nm×30 nm, $U=-0.9$ V, $I=0.21$ nA) showing the domain boundaries.

$$\begin{bmatrix}\mathbf{b}_1\\ \mathbf{b}_2\end{bmatrix}=\begin{bmatrix}4 & 1\\ 1 & 3\end{bmatrix}\begin{bmatrix}\mathbf{a}_1\\ \mathbf{a}_2\end{bmatrix}.$$

STM results at 77 K indicate the same superstructure. In many cases, the difference in thermal expansion coefficient of the metal substrate and the organic adlayers leads to structural transition with temperature. However, in our experiments, there is no obvious difference between the structure at room temperature and that at 77 K.

Figure 2(b) shows the structural relation between the molecular superstructure $(\mathbf{b}_1,\mathbf{b}_2)$ and the Ag(110) substrate lattice $(\mathbf{a}_1,\mathbf{a}_2)$. The unit cell vectors of the Ag(110) substrate are $\mathbf{a}_1=2.889$ Å and $\mathbf{a}_2=4.086$ Å. According to the above matrix, the unit cell vectors of the perylene superstructure are $\mathbf{b}_1=16$ Å and $\mathbf{b}_2=15$ Å with an enclosed angle of $\Gamma=57°$. The enclosed angle between $\mathbf{b}_1$ and $\mathbf{a}_1$ is $\oslash=19°$. The adsorption sites of perylene molecules relative to the Ag atoms of the substrate are arbitrarily chosen in Fig. 2(b).

Figure 3(a) shows an STM image of the highly ordered perylene monolayer. There is only one domain in the entire scanning area. Our STM experiments show that the size of single domain is far larger than 115 nm, which is close to the upper limit of the scanning range for molecular resolution; that is, the density of domain boundary is rather low. Figure 3(b) shows the domain boundaries. Even near these boundaries, the highly ordered arrangement is maintained, and only several molecules are mismatched.

To identify the specific adsorption sites of perylene molecules on Ag(110) surface, first-principles calculation has been conducted. First-principles calculations were carried out using density functional theory (DFT), the Perdew-Wang (PW91) generalized gradient approximation (GGA) for exchange-correlation energy,[40] Vanderbilt ultrasoft pseudopotentials[41] and a plane wave basis set as implemented in the Vienna *ab initio* simulation package (VASP) code.[41,42]

First, we considered the possible adsorption configurations of individual perylene molecules on Ag(110). Individual perylene molecules prefer the "lying-flat" adsorption mode with their long axis parallel to the $[1\bar{1}0]$ direction of silver substrate.[43] Seven typical adsorption configurations

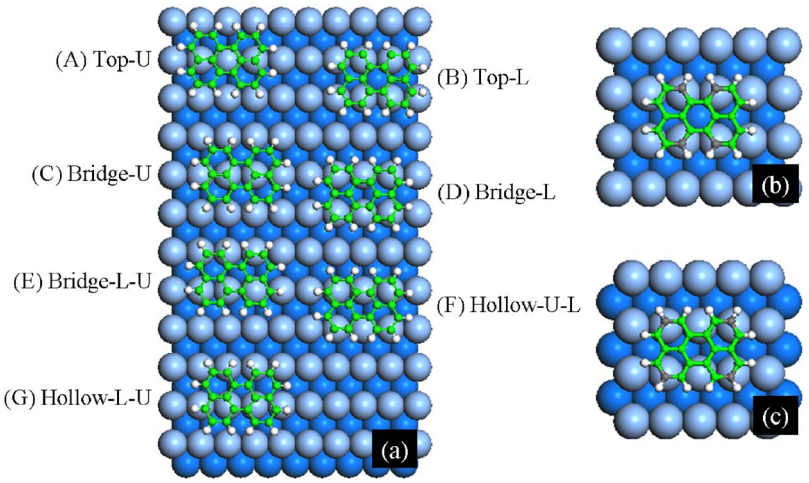

FIG. 4. (Color online) Schematic diagrams for the optimization of perylene supercells on Ag(110). (a) Seven supposed adsorption configurations of single molecule with different adsorption sites (A–F). They are all adsorbed in "lying-flat" mode with their long axis along the $[1\bar{1}0]$ direction of the Ag(110) surface. *U* and *L* represent the upper and lower atoms in the first layer of the Ag(110) surface, respectively. (b) The molecular configuration of the optimized S-B perylene supercell. (c) The molecular configuration of the optimized S-D perylene supercell.

exist with different adsorption sites, as shown in Fig. 4(a).[44] Second, we conducted energy optimization of a perylene supercell. The seven types of supercells from S-A to S-G are based on the seven configurations of individual molecules from A to G. The results indicate that, for all seven types of supercells, the molecular plane is approximately parallel to the silver surface with a slight bend and the long axis of molecules is approximately parallel to the $[1\bar{1}0]$ direction. The slight offset of optimized molecular positions from the original positions is ascribed to the spontaneous symmetry broken of the system. The molecule-substrate distances, defined as the height difference between the average height of C atoms in perylene molecules and that of Ag atoms in the first layer, are 3.10 Å for S-B, 3.14 Å for S-D, 3.21 Å for S-F, 3.27 Å for S-E, and over 3.40 Å for the other three supercells. In the S-B and S-D, the C-Ag bond lengths of the four C atoms, indicated by the gray color in Figs. 4(b) and 4(c), are smaller than those of the other C atoms are in the same molecule, which leads to the slight bend of the molecular plane. The average C-Ag bond lengths of the four C atoms shown in gray are 3.05 and 3.07 Å for S-B and S-D, respectively. These values are between the bond length of the typical C-Ag covalent bond and that of the typical van der Waals bond, which indicates that the secondary chemical interactions between molecules and substrate occur via these closely bonded C atoms in the S-B and S-D. The adsorption energy values are 311 meV for S-B, 304 meV for S-D, around 270 meV for S-E and S-F, and below 200 meV for the other three supercells, respectively. So the adsorption energy decreases with the increase of molecule-substrate distance. The S-B has the highest adsorption energy and the smallest molecule-substrate distance, thereby is the most stable configuration for perylene on Ag(110), as shown in Fig. 5(a).

In order to check the validity of our calculation, we simulated the STM image of fully relaxed stable structure S-B by calculating the density of states (DOS) using the Tersoff-Hamann approach.[45] Typical tunneling conditions in our STM experiments, $U=-1.2$ V and $I=0.13$ nA, are used in our simulation. The simulated STM image, as shown in Fig. 5(b), is in good agreement with the STM image obtained in our experiments [see Fig. 5(c)].

The growth of perylene monolayer on Ag(110), as described above, represents one typical growth mode for organic thin films. The growth process is inherently a nonequilibrium phenomenon governed by the competition between kinetics and thermodynamics. The diffusion of a molecule on a flat terrace is by far the most important kinetic process in monolayer growth. The surface diffusion coefficient D is related with the site to site hopping rate of a molecule k_s by $D=a^2k_s$, where a is the effective hopping distance between sites and $k_s \propto \exp(-V_s/k_BT)$, where V_s is the potential-energy barrier from site to site, T is the substrate temperature, and k_B is the Boltzmann constant. In our experiment, if perylene molecules are deposited on the Ag(110) surface at a constant deposition rate F, then the ratio D/F determines the average distance that a perylene molecule has to travel to be localized at its final adsorption sites before the coverage is increased up to one monolayer, because perylene molecules do not aggregate into molecular islands in the submonolayer regime. The ratio of deposition to diffusion rate D/F is thus the key parameter characterizing growth kinetics. In the case of large values of D/F, growth occurs close to equilibrium conditions; that is, the molecules have enough time to ex-

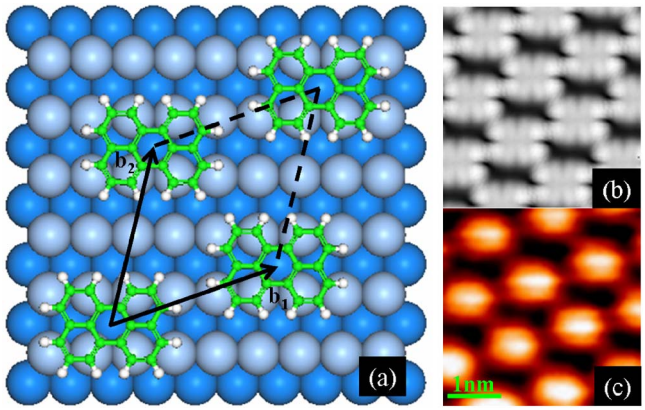

FIG. 5. (Color online) (a) The model of the favorable superstructure S-B obtained with energy optimization. (b) Simulated STM image (−1.2 V) of perylene S-B superstructure. (c) Experimental STM image (4 nm×4 nm, $U=-1.2$ V, $I=0.13$ nA) of perylene superstructure.

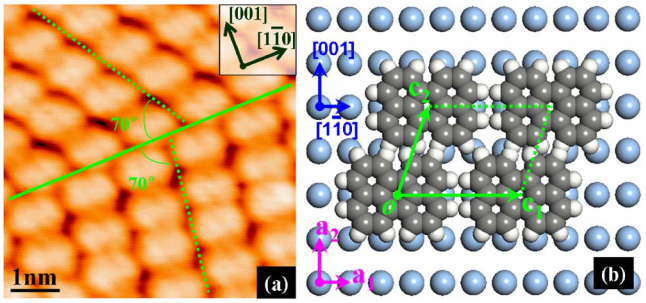

FIG. 6. (Color online) (a) The STM image (6 nm×6 nm, $U=-0.8$, $I=0.17$ nA) of the modal metastable structure. (b) Supposed model of the modal metastable structure.

plore the potential energy surface so that the system reaches a minimum energy configuration. On the contrary, in the case of small values of D/F, the growth is essentially determined by kinetics; individual processes, especially those leading to metastable structures, are increasingly important.

The perylene superstructure is sensitive to growth conditions. The uniform monolayer superstructure obtained in our experiment is different from those reported in Ref. 30, which is the result of different growth conditions. The deposition rate was about 4×10^{-3} ML/min for the preparation of the uniform monolayer discussed above. The growth with a higher deposition rate, about 1×10^{-2} ML/min, leads to the formation of many metastable structures. All the observed metastable structures are locally distributed in the monolayer, and cannot be detected from LEED patterns. These structures are very complex, and difficult to be well characterized one by one. Figure 6(a) shows the STM image of one modal structure including two domains due to the twofold symmetry of the Ag(110) substrate. By analyzing a large number of STM images of the modal structure and those of atomic-resolution uncovered Ag(110) surface, the modal structure is determined as follows:

$$\begin{bmatrix} \mathbf{c}_1 \\ \mathbf{c}_2 \end{bmatrix} = \begin{bmatrix} 4 & 0 \\ 1 & 2 \end{bmatrix} \begin{bmatrix} \mathbf{a}_1 \\ \mathbf{a}_2 \end{bmatrix}$$

Fig. 6(b) shows the structural relation between the modal metastable structure $(\mathbf{c}_1,\mathbf{c}_2)$ and the substrate lattice $(\mathbf{a}_1,\mathbf{a}_2)$. According to this model, the unit cell vectors of the perylene superstructure are $\mathbf{c}_1=11.6$ Å and $\mathbf{c}_2=8.7$ Å with an enclosed angle of $\Gamma=70.5°$. The measured enclosed angle directly from STM images is around 70 ° which is in good agreement with this model. In this model, the molecular configuration is assumed as "flat-flying" with respect to the substrate and molecular long axis parallel to $[1\bar{1}0]$ direction, which is reasonable according to the theoretical calculations;[43] however, the specific adsorption sites are arbitrarily chosen. This modal structure, with an average size around 10nm, is interspersed in the monolayer by an average distribution density of about 5 per 100 nm×100 nm.

The high sensitivity of the perylene monolayer structure to the growth conditions is due to the fact that the difference in adsorption energy between the stable structure and the metastable structures is rather small. We attribute this difference to the weak intermolecular and molecule-substrate interactions. Therefore, in order to fabricate monolayers with uniform structure, growth conditions should be controlled precisely. Because of this, molecular self-assembly in weakly interacting system is full of challenges. On the other hand, for a weakly interacting system, the weak intermolecular interaction and molecule-substrate interaction facilitate the unusually low density of domain boundaries in monolayers, which results in good performance in OFETs and OLEDs.

IV. CONCLUSIONS

In summary, we have systematically studied the interface between perylene and Ag(110) from very low coverage to monolayer coverage by combining STM, LEED, and first-principles calculations. The growth mode of the perylene/Ag(110) interface is typical for weakly interacting systems. Due to the weakness of both the molecule-substrate and molecule-molecule interactions, perylene shows poor self-assembly ability as discussed above. However, by finely controlling the growth conditions, we succeeded in the fabrication of the perylene monolayer of high quality. The present work indicates that it is feasible to realize the exquisite control over the formation of nanoscale structures in weakly interacting systems.

ACKNOWLEDGMENTS

This work was supported in part by the National Science Foundation of China, the National "863" and "973" projects, and the Supercomputing Center, CNIC, CAS.

*Electronic address: hjgao@aphy.iphy.ac.cn

[1] S. Lukas, G. Witte, and C. Wöll, Phys. Rev. Lett. **88**, 028301 (2002).
[2] F. Rosei, M. Schunack, P. Jiang, A. Gourdon, E. Lægsgaard, I. Stensgaard, C. Joachim, and F. Besenbacher, Science **296**, 328 (2002).
[3] Y. L. Wang, W. Ji, D. X. Shi, S. X. Du, C. Seidel, Y. G. Ma, H.-J. Gao, L. F. Chi, and H. Fuchs, Phys. Rev. B **69**, 075408 (2004).
[4] J. A. Theobald, N. S. Oxtoby, M. A. Phillips, N. R. Champness, and P. H. Beton, Nature (London) **424**, 1029 (2003).
[5] M. Böhringer, K. Morgenstern, W. D. Schneider, R. Berndt, F. Mauri, A. De Vita, and R. Car, Phys. Rev. Lett. **83**, 324 (1999).
[6] A. Kahn, N. Koch, and W. Gao, J. Polym. Sci., Part B: Polym. Phys. **41**, 2529 (2003).
[7] G. Witte and C. Wöll, J. Mater. Res. **19**, 1889 (2004).
[8] H.-J. Gao, K. Sohlberg, Z. Q. Xue, H. Y. Chen, S. M. Hou, L. P. Ma, X. W. Fang, S. J. Pang, and S. J. Pennycook, Phys. Rev. Lett. **84**, 1780 (2000).
[9] H. Hoppe and N. S. Sariciftci, J. Mater. Res. **19**, 1924 (2004).
[10] G. Horowitz, J. Mater. Res. **19**, 1946 (2004).

[11] W. Clemens, W. Fix, J. Ficker, A. Knobloch, and A. Ullmann, J. Mater. Res. **19**, 1963 (2004).
[12] J. R. Sheats, J. Mater. Res. **19**, 1974 (2004).
[13] W. R. Salaneck and M. Fahlman, J. Mater. Res. **19**, 1917 (2004).
[14] B. Crone, A. Dodabalapur, Y. Y. Lin, R. W. Filas, Z. Bao, A. LaDuca, R. Sarpeshkar, H. E. Katz, and W. Li, Nature (London) **403**, 521 (2000).
[15] E. J. Meijer, D. M. Deleeuw, S. Setayesh, E. van Veenendaal, B.-H. Huisman, P. W. M. Blom, J. C. Hummelen, U. Scherf, and T. M. Klapwijk, Nat. Mater. **2**, 678 (2003).
[16] L. Schmidt-Mende, A. Fechtenkötter, K. Müllen, E. Moons, R. H. Friend, and J. D. MacKenzie, Science **293**, 1119 (2001).
[17] P. R. L. Malenfant, C. D. Dimitrakopoulos, J. D. Gelorme, L. L. Kosbar, and T. O. Graham, Appl. Phys. Lett. **80**, 2517 (2002).
[18] P. Peumans, S. Uchida, and S. R. Forrest, Nature (London) **425**, 158 (2003).
[19] R. H. Friend, R. W. Gymer, A. B. Holmes, J. H. Burroughes, R. N. Marks, C. Taliani, D. D. C. Bradley, D. A. Dos Santos, J. L. Brédas, M. Lögdlund, and W. R. Salaneck, Nature (London) **397**, 121 (1999).
[20] C. G. Zeng, B. Wang, B. Li, H. Q. Wang, and J. G. Hou, Appl. Phys. Lett. **79**, 1685 (2001).
[21] T. Yokoyama, S. Yokoyama, T. Kamikado, Y. Okuno, and S. Mashiko, Nature (London) **413**, 619 (2001).
[22] M. Eremtchenko, D. Bauer, J. A. Schaefer, and F. S. Tautz, J. Mater. Res. **19**, 2028 (2004).
[23] R. Nowakowski, C. Seidel, and H. Fuchs, Phys. Rev. B **63**, 195418 (2001).
[24] M. Eremtchenko, J. A. Schaefer, and F. S. Tautz, Nature (London) **425**, 602 (2003).
[25] B. A. Jones, M. J. Ahrens, M. H. Yoon, A. Facchetti, T. J. Marks, and M. R. Wasielewski, Angew. Chem., Int. Ed. **43**, 6363 (2004).
[26] Y. Toda and H. Yanagi, Appl. Phys. Lett. **69**, 2315 (1996).
[27] Th. Basché and W. E. Moerner, Nature (London) **355**, 335 (1992).
[28] Th. Christ, F. Petzke, P. Bordat, A. Herrmann, E. Reuther, K. Müllen, and Th. Bashé, J. Lumin. **98**, 23 (2002).
[29] X. D. Liu, V. Kaiser, M. Wuttig, and T. Michely, J. Cryst. Growth **269**, 542 (2004).
[30] C. Seidel, R. Ellerbrake, L. Gross, and H. Fuchs, Phys. Rev. B **64**, 195418 (2001).
[31] Q. Chen, T. Rada, A. McDowall, and N. V. Richardson, Chem. Mater. **14**, 743 (2002).
[32] S. Sohnchen, K. Hanel, A. Birkner, G. Witte, and C. Wöll, Chem. Mater. **17**, 5297 (2005).
[33] A. R. McGhie, A. F. Garito, and A. J. Heeger, J. Cryst. Growth **22**, 295 (1974).
[34] C. Seidel, J. Poppensieker, and H. Fuchs, Surf. Sci. **408**, 223 (1998).
[35] J. I. Pascual, J. J. Jackiw, K. F. Kelly, H. Conrad, H.-P. Rust, and P. S. Weiss, Phys. Rev. B **62**, 12632 (2000).
[36] S. J. Stranick, M. M. Kamna, and P. S. Weiss, Science **266**, 99 (1994).
[37] X. Chen, I. R. Frank, and R. J. Hamers, J. Vac. Sci. Technol. B **14**, 1136 (1996).
[38] L. E. Urbach, K. L. Percival, J. M. Hicks, E. W. Plummer, and H.-L. Dai, Phys. Rev. B **45**, 3769 (1992).
[39] K.-M. Ho, B. N. Harmon, and S. H. Liu, Phys. Rev. Lett. **44**, 1531 (1980).
[40] J. P. Perdew, J. A. Chevary, S. H. Vosko, K. A. Jackson, M. R. Pederson, D. J. Singh, and C. Fiolhais, Phys. Rev. B **46**, 6671 (1992).
[41] G. Kresse and J. Furthmüller, Phys. Rev. B **54**, 11169 (1996).
[42] G. Kresse and J. Hafner, Phys. Rev. B **47**, R558 (1993).
[43] W. Ji, L. Gao, Z. T. Deng, and H. J. Gao (unpublished).
[44] We define the sites top-U, top-L, bridge-U, bridge-L, bridge-L-U, hollow-U-L, and hollow-L-U as sites A–G, respectively. Each configuration is defined by the adsorption sites. For example, A denotes the configuration that the center of a perylene molecules is located over the Ag atoms of the upper layer of the Ag(110) substrate.
[45] J. Tersoff and D. R. Hamann, Phys. Rev. B **31**, 805 (1985).